A study of the dissociation of CH3CH2SH+ by collisional activation: Evidence of nonstatistical behavior

Y.-J. Chen, S. Stimson, P. T. Fenn, C. Y. Ng, Wai-Kee Li et al.

Citation: J. Chem. Phys. **108**, 8020 (1998); doi: 10.1063/1.476241
View online: http://dx.doi.org/10.1063/1.476241
View Table of Contents: http://jcp.aip.org/resource/1/JCPSA6/v108/i19
Published by the American Institute of Physics.

A study of the dissociation of $CH_3CH_2SH^+$ by collisional activation: Evidence of nonstatistical behavior

Y.-J. Chen, S. Stimson, P. T. Fenn, and C. Y. Ng[a)]
Ames Laboratory, United States Department of Energy, Ames, Iowa and Department of Chemistry, Iowa State University, Ames, Iowa 50011

Wai-Kee Li
Department of Chemistry, The Chinese University of Hong Kong, Shatin, N. T., Hong Kong

N. L. Ma[b)]
Department of Applied Biology and Chemical Technology, Hong Kong Polytechnic University, Hung Ham, Hong Kong

(Received 12 January 1998; accepted 9 February 1998)

The absolute total cross sections for $CH_3CH_2^+$, $C_2H_4^+$, $C_2H_3^+$, CH_3^+, $CH_2SH^+(CH_3S^+)$, $CH_2S^+(HCSH^+)$, $CHS^+(CSH^+)$, and H_2S^+ produced by the collision-induced dissociation (CID) reaction of $CH_3CH_2SH^+ + Ar$ have been measured in the center-of-mass collision energy ($E_{c.m.}$) range of 1–42 eV. Using the charge transfer probing technique, we found that the mass 47 product ions have overwhelmingly the CH_2SH^+ structure. The onsets for $CH_3CH_2^+$, $C_2H_4^+$, $C_2H_3^+$, CH_2SH^+, H_2S^+, and CH_3^+ are consistent with their corresponding thermochemical thresholds. The formation of the higher energy channels $CH_3CH_2^+ + SH$ and $CH_3 + CH_2SH^+$, which involve the C–S and C–C bond scissions, are found to dominate in the entire $E_{c.m.}$ range. The lower energy channel corresponding to the formation of $CH_3CHSH^+ + H$ is not found. The strong preference observed for the formation of the higher energy channels is in accord with the conclusion obtained in the recent CID study of CH_3SH^+, providing evidence that the CID of $CH_3CH_2SH^+$ is also nonstatistical. The high yields of $CH_3CH_2^+ + SH$ and $CH_2SH^+ + CH_3$ are attributed to the more efficient translational to vibrational energy transfer for the low frequencies C–S and C–C stretching modes than for the high frequencies C–H and S–H stretching modes, along with the weak couplings between these low and high frequencies vibrational modes of $CH_3CH_2SH^+$. The relative abundances of product ions formed by the single-photon ionization of CH_3CH_2SH were also measured for comparison with the CID results. The $CH_3CHSH^+ + H$ channel is observed in the photoionization of CH_3CH_2SH. Similar to the finding in the photoionization of CH_3SH, the relative abundances of fragment ions formed in the photoionization of CH_3CH_2SH are in qualitative accord with statistical predictions. To rationalize the dissociation mechanisms of $CH_3CH_2SH^+$, we have also performed *ab initio* calculations to locate the possible transition structures for the observed dissociation channels. © *1998 American Institute of Physics.* [S0021-9606(98)00119-6]

I. INTRODUCTION

We have recently examined the collision-induced dissociation (CID) reaction of $CH_3SH^+ + Ar$.[1,2] The absolute cross section for $CH_3^+ + SH$ is found to be significantly higher than that for $CH_2SH^+ + H$. Since the CH_3^+–SH bond is considerably stronger than the H-CH_2SH^+ bond, this observation suggests that the CID of CH_3SH^+ is nonstatistical, and is thus bond selective. However, this conclusion is contrary to the results observed in the dissociation of CH_3SH^+ excited by photoionization (PI) (Ref. 3) and charge exchange.[4] The breakdown diagrams for the unimolecular dissociation of CH_3SH^+ activated by PI and charge exchange are in qualitatively agreement with the statistical quasiequilibrium theory (QET).[2–4]

Motivated by the striking differences in the CH_3SH^+ dissociation product branching ratios observed between the CID experiment and the PI and charge exchange studies, we have further examined the CID of $CH_3CH_2SH^+$. The latter ion contains an extra C–C bond compared to CH_3SH^+. In order to compare the dissociation mechanisms activated by collision and PI, we have also performed a PI mass spectrometric study of CH_3CH_2SH. The structures of the mass 47 (CH_2SH^+ or CH_3S^+) product ions formed in the CID reaction of $CH_3CH_2SH^+ + Ar$ and in the PI of CH_3CH_2SH have also been probed by using the charge exchange probing method.[2]

The reactant $CH_3CH_2SH^+$ ions in the present CID experiment are prepared by PI of CH_3CH_2SH in the threshold region. By using a sufficiently high photon energy resolution, the $CH_3CH_2SH^+$ ion can be formed in its ground vibronic state. Since the CH_3CH_2SH sample is introduced by supersonic expansion into the ion source and PI is known to favor a small change in rotational quantum numbers, the re-

a)Author to whom correspondence should be addressed: CYNG@AMESLAB.GOV
b)Present address: Department of Chemistry, National University of Singapore, 10 Kent Ridge Crescent, Singapore, 119260.

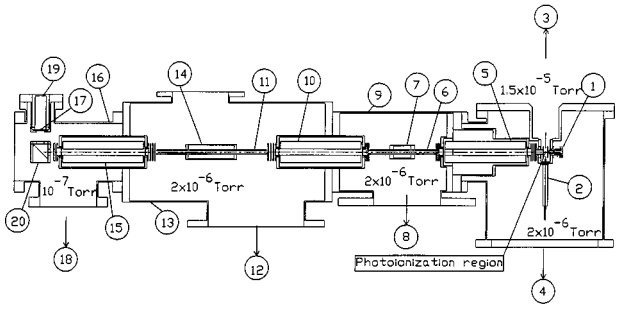

FIG. 1. Schematic diagram of the TQDO apparatus. (1) Electron impact ionization ion source, (2) atomic or molecular nozzle beam, (3) to freon-trapped 6 in. diffusion pump (DP), (4) to liquid-nitrogen (LN_2)-trapped 6 in. DP, (5) reactant QMS, (6) lower RF octopole ion guide, (7) lower RFOIGGC, (8) to LN_2-trapped 6 in. DP, (9) the lower RF octopole ion guide chamber, (10) middle QMS, (11) upper RF octopole ion guide, (12) to LN_2-trapped 4 in. DP, (13) upper RF octopole ion guide chamber, (14) upper RFOIGGC, (15) product QMS, (16) detector chamber, (17) plastic scintillator window, (18) to LN_2-trapped 2 in. DP, (19) photomultiplier tube, (20) aluminum ion target.

actant ion beam thus formed should also be rotationally cold.

On the basis of the self-consistent-field molecular orbital calculation using the 4-31G basis set,[5] the main electronic configuration for CH_3CH_2SH is predicted to be $\ldots.(11a')^2(3a'')^2(12a')^2(13a')^2(4a'')^2$. The highest $4a''$ orbital is a nonbonding orbital localized mostly at the S atom. The $13a'$ orbital has mainly the σ(C–S) bond in character, while the $12a'$ orbital is associated with the σ(S–H) and σ(C–C) bonds. The first to fifth photoelectron bands observed in previous He I photoelectron spectroscopic studies[5] have been assigned correspondingly to the removal of an electron from the $4a''$, $13a'$, $12a'$, $3a''$, and $11a'$ orbitals of CH_3CH_2SH with respective vertical ionization energies (IEs) of 9.58, 11.87, 13.43, 14.62, and 16.82 eV.[5]

II. EXPERIMENT

The arrangement of the triple–quadrupole double–octopole (TQDO) PI ion–molecule reaction apparatus (Fig. 1) and procedures used to perform state-selected absolute total cross section measurements have been described in detail previously.[6–8] The TQDO apparatus essentially consists of, in sequential order, a vacuum ultraviolet (VUV) PI ion source, an electron impact ion source (1), a reactant quadrupole mass spectrometer (QMS) (5), a lower radio frequency (RF) octopole ion guide reaction gas cell (RFOIGGC) [(6)+(7)], a middle QMS (10), an upper RFOIGGC [(11)+(14)], a product QMS (15), and a modified[9] Daly-type scintillation ion detector [(17)+(19)+(20)]. The electron impact ion source is not used in this experiment. The TQDO apparatus is partitioned into five chambers which are separately evacuated by liquid nitrogen or freon-trapped diffusion pumps.

The PI ion source consists of a 0.2 m VUV monochromator (McPherson 234), a hydrogen discharge lamp, and a photoelectric VUV light detector. The recent high resolution nonresonant two-photon pulsed field ionization photoelectron (N2P-PFI-PE) study of CH_3CH_2SH near the ionization threshold yields a value of 9.2927 ± 0.0006 eV (1334 ± 0.08 Å) for the IE of CH_3CH_2SH.[10] The N2P-PFI-PE spectrum also reveals a vibrational progression corresponding to excitation of the C–S stretching mode ($\nu_4^+ = 628\ cm^{-1}$) of $CH_3CH_2SH^+$. In the present experiment, CH_3CH_2SH is introduced into the PI source as a free jet formed by supersonic expansion through a nozzle with a diameter of 75 μm at a stagnation pressure of ≈ 120 Torr. By setting the PI wavelength at 1333 Å and a wavelength resolution of 5 Å [full-width-at-half-maximum (FWHM)], the $CH_3CH_2SH^+$ reactant ions were formed in their ground vibronic states. The rotational temperature of $CH_3CH_2SH^+$ thus formed is expected to be <150 K, characteristic of the neutral CH_3CH_2SH jet. We note that finite vibrational excitations of $CH_3CH_2SH^+$ due to the thermal population of low frequency vibrational modes of CH_3CH_2SH may not be efficiently relaxed by the mild beam expansion employed in this experiment.

For absolute total cross section measurements, the reactant $CH_3CH_2SH^+$ ions were extracted and guided by the lower QMS (operated in the RF only mode) and the lower RF octopole ion guide to the middle QMS. The middle QMS, functioning as a mass filter, passed only the desired $CH_3CH_2SH^+$ ions to the upper RFOIGGC, where collision-activated dissociation occurred with Ar. The pressure of Ar in the upper RFOIGGC was monitored with a MKS Baratron manometer, and maintained at $2-3\times10^{-4}$ Torr. In this pressure range, the CID product ion intensity was found to have a linear dependence on the Ar gas cell pressure. The reactant ions and the product ions formed in the upper RFOIGGC were then mass selected by the product QMS and detected with the modified Daly-type scintillation ion detector.

The reactant ion beam energies were determined by the retarding potential method, using the upper octopole ion guide to retard the reactant $CH_3CH_2SH^+$ ions. The retarding potential curve thus obtained was differentiated to yield the most probable laboratory kinetic energy (E_{lab}) of the reactant ions and the FWHM of the kinetic energy distribution. The E_{lab} resolution for $CH_3CH_2SH^+$ achieved in this experiment was ± 0.2 eV as measured by the FWHM of the E_{lab} distribution. The center-of-mass collision energy ($E_{c.m.}$) resolution was ± 0.08 eV (FWHM). The collection efficiencies for reactant and product ions were maximized at each $E_{c.m.}$ by optimizing the voltage settings applied to the ion lenses, the octopole ion guides, and the QMS's.

To probe the structure of the mass 47 ions formed in the CID reaction of $CH_3CH_2SH^+ + Ar$, we used both the lower and upper RFOIGGCs. Reactant $CH_3CH_2SH^+$ ions prepared by PI of CH_3CH_2SH were first selected by the reactant QMS to enter the lower RFOIGGC, where the CID reaction $CH_3CH_2SH^+ + Ar$ took place. The Ar gas cell pressure used was 5×10^{-4} Torr. The mass 47 product ions thus formed in the $E_{c.m.}$ range of 4.5–6.5 eV were selected by the middle QMS and guided into the upper RFOIGGC, in which the structure for the mass 47 ions was probed by the charge transfer reaction with benzene (C_6H_6) at $E_{c.m.}<0.4$ eV. Charge transfer product $C_6H_6^+$ ions, if formed, were detected by the product QMS. The C_6H_6 pressure used in the upper gas cell was 3×10^{-4} Torr. The IEs for CH_3S, CH_2SH, and

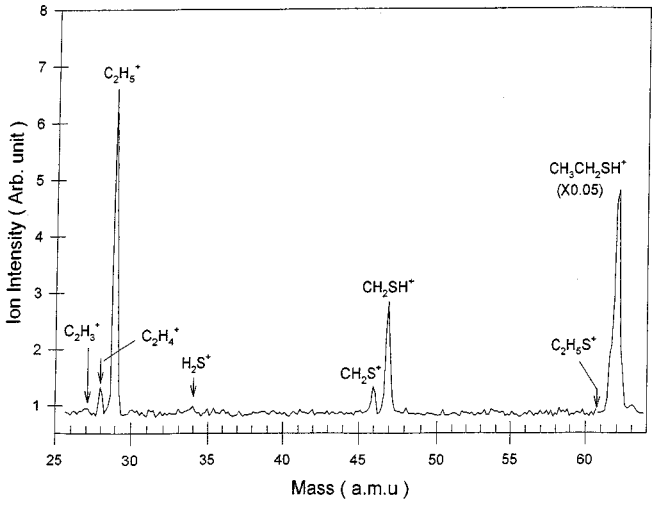

FIG. 2. Mass spectrum in the mass range of $m/e=25-64$ amu for the CID reaction of $CH_3CH_2SH^+ + Ar$ obtained at $E_{c.m.}=5.3$ eV. The mass peak for $m/e=62$ amu has been scaled by a factor of 0.05. Note that the mass peak $m/e=61$ corresponding to CH_3CHSH^+ is absent in the spectrum.

C_6H_6 are known to be 9.2649 ± 0.0010 eV,[11] 7.536 ± 0.003 eV,[12] and 9.243842 ± 0.000006 eV,[13] respectively. Using these IE values, we calculated that the charge transfer reaction (1) for CH_3S^+ is slightly exothermic by 0.0211 eV, whereas the charge transfer reaction (2) for CH_2SH^+ is endothermic by 1.708 eV. The ΔH_0^0 values given in reactions (1) and (2) are the corresponding heats of reaction at 0 K,

$$CH_3S^+ + C_6H_6 \rightarrow CH_3S + C_6H_6^+ \quad \Delta H_0^0 = -0.0211 \text{ eV}, \tag{1}$$

$$CH_2SH^+ + C_6H_6 \rightarrow CH_2SH + C_6H_6^+ \quad \Delta H_0^0 = 1.708 \text{ eV}. \tag{2}$$

Since near-resonant charge transfer reactions usually have large cross sections, we should observe the formation of $C_6H_6^+$ if the mass 47 ions have the CH_3S^+ structure, while the charge transfer cross section should be negligibly small if CH_2SH^+ ions are produced in the CID reaction of $CH_3CH_2SH^+ + Ar$.

It is known that CH_2SH^+ ions are produced at the onset by the PI of CH_3SH.[3] This conclusion is based on the fact that the thermochemical threshold of $\Delta H_0^0=11.541$ eV for process (3) is very close to the appearance energy (AE) of ≈ 11.55 eV for the mass 47 ion observed in the dissociative PI of CH_3SH,

$$CH_3SH + h\nu \rightarrow CH_2SH^+ + H + e, \quad \Delta H_0^0 = 11.541 \text{ eV}. \tag{3}$$

The formation of CH_2SH^+ by process (3) has been further confirmed by Fenn *et al.* using benzene as the charge transfer probing reactant.[2] The latter experiment can be taken as a validation of the charge transfer probing technique used here for the structural identification of the mass 47 ions (CH_2SH^+ or CH_3S^+) formed in the PI and CID reactions.

The data acquisition for the TQDO apparatus has recently been upgraded to be controlled by a Pentium PC system.[14] This improvement allows computer control of the QMS and monochromator scans, the voltage settings applied to individual components of the ion optics system, the reactant ion kinetic energy determination, and the background corrections in absolute total cross section measurements. The procedures outlined above were conducted mostly in an automatic mode.

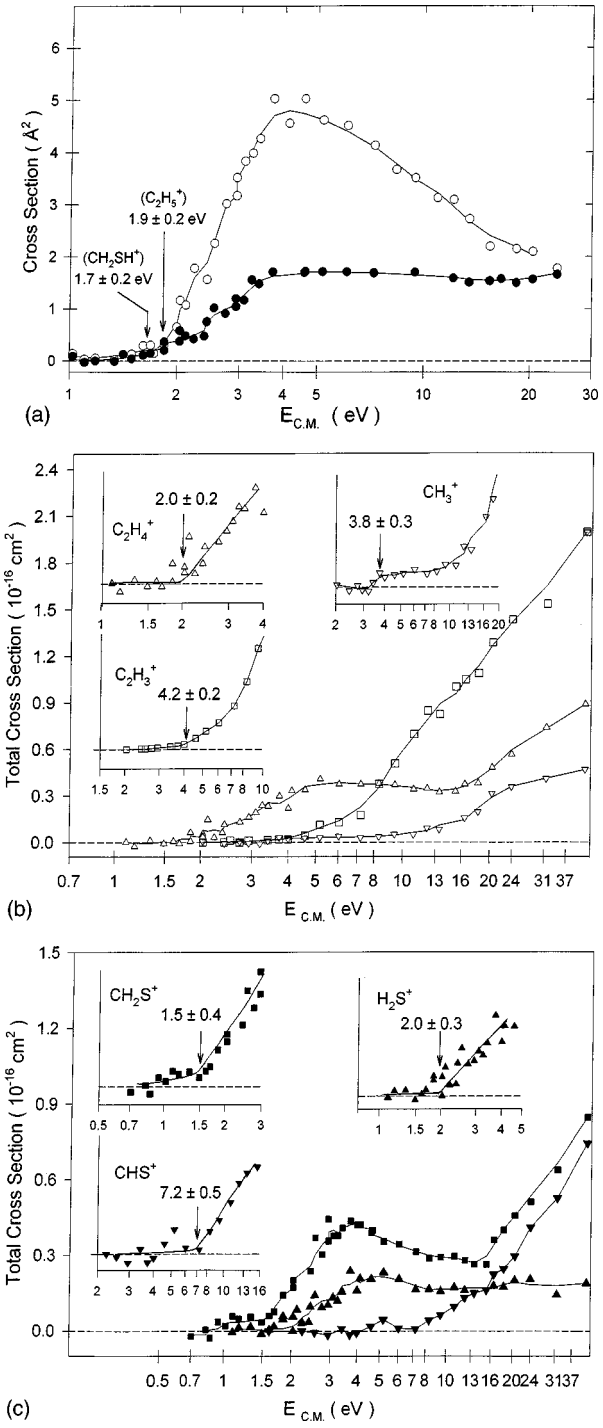

FIG. 3. Absolute total cross section curves for (a) CH_2SH^+ (CH_3S^+) (●) and $CH_3CH_2^+$ (○); (b) $C_2H_4^+$ (△), $C_2H_3^+$ (□), and CH_3^+ (▽); and (c) CH_2S^+ (■), H_2S^+ (▲), and HCS^+ (▼) formed in the CID reaction of $CH_3CH_2SH^+ + Ar$ at $E_{c.m.}=0.5-42$ eV.

The ethanethiol and benzene were obtained from Aldrich Chemical Co. and Fisher Scientific with purities of 99.5%

TABLE I. Appearance energies (AEs) and Δ (PI)[a] values for $C_2H_5^+$, $C_2H_4^+$, $C_2H_3^+$, $CH_2SH^+(CH_3S^+)$, CH_2S^+, CHS^+, CH_3^+, and H_2S^+ formed in the CID of $CH_3CH_2SH^+$ and PI of CH_3CH_2SH, respectively.

Product ions	AE(CID)[b] (eV)	Δ (PI) (eV)
CH_3CHSH^+	⋯	1.47±0.06
$CH_3CH_2^+$	1.9±0.2	2.0±0.06
$C_2H_4^+$	2.0±0.2	2.0±0.06
$C_2H_3^+$	4.2±0.2	⋯
CH_2SH^+	1.7±0.2	1.73±0.06
CH_2S^+	1.5±0.4	1.42±0.06
CHS^+	7.2±0.5	⋯
CH_3^+	3.8±0.3	⋯
H_2S^+	2.0±0.3	1.93±0.06

[a]This work. Δ(PI)=AE(PI)−IE(CH_3SH), where AE(PI) is the AE determined in the PI of CH_3CH_2SH.
[b]This work. Appearance energy determined in the CID study of $CH_3CH_2SH^+$+Ar. The uncertainties represent the precision of the measurements.

and 99.9%, respectively. The Ar gas is from Air Products and has a purity of 99.998%.

III. RESULTS AND DISCUSSION

A. Absolute total cross section and identification of CID product channels

Figure 2 depicts the mass spectrum observed for the CID reaction of $CH_3CH_2SH^+$+Ar at $E_{c.m.}$=5.3 eV by scanning the product quadrupole mass spectrometer, showing that $C_2H_5^+$ and $CH_2SH^+(CH_3S^+)$ are the major product ions. The product ions observed in the CID reaction of $C_2H_5SH^+$+Ar are $C_2H_5^+$, $C_2H_4^+$, $C_2H_3^+$, CH_2SH^+, CH_2S^+, H_2S^+, CHS^+, and CH_3^+. We note that the mass peaks for CHS^+ and CH_3^+ are not shown in Fig. 2.

The absolute total cross section for the dominant product ions $C_2H_5^+$ and $CH_2SH^+(CH_3S^+)$ in the $E_{c.m.}$ range of 1–37 eV are plotted in Fig. 3(a). The cross sections of $C_2H_5^+$ and $CH_2SH^+(CH_3S^+)$ exhibit a maximum at $E_{c.m.}$=3–7 eV. The maximum cross section for $C_2H_5^+$ is about 5 Å^2, which is more than three times higher than the maximum cross section of 1.8 Å^2 for $CH_2SH^+(CH_3S^+)$. The cross section curves for the minor product ions are depicted in Fig. 3(b) for $C_2H_4^+$, $C_2H_3^+$, and CH_3^+ and in Fig. 3(c) for CH_2S^+, CHS^+, and H_2S^+. The onsets for these minor product ions are found to rise very gradually as $E_{c.m.}$ is increased. The cross section of $C_2H_3^+$ increases rapidly at $E_{c.m.}>8$ eV and reaches ≈2 Å^2 at $E_{c.m.}\approx 30$ eV, a value similar to the cross sections for $C_2H_5^+$ and CH_2SH^+ (and/or CH_3S^+). The cross sections for other minor product ions are <1 Å^2 in the entire $E_{c.m.}$ range.

One of the most important pieces of information obtained in a low energy CID study is the AEs of the product ions, from which upper limits of the bond dissociation energies at 0 K (D_0) involved can be calculated. The AE(CID) values for $C_2H_5^+$, $C_2H_4^+$, $C_2H_3^+$, CH_3^+, CH_2SH^+, CH_2S^+, CHS^+, and H_2S^+ determined by the cross-section curves are listed in Table I. At $E_{c.m.}$ below these AE(CID) values, the intensities for the corresponding product ions are at the background level. These AE(CID) values represent upper limits for the true thermochemical thresholds of the processes involved. Using the current recommended thermochemical data[3,10–24] listed in Table II, we have calculated the ΔH_0^0 values for the reactions possibly responsible for the observed CID product ions. All atomic and molecular species in the following reactions are assumed to be in their ground states:

$$CH_3CH_2SH^+ + Ar \rightarrow CH_3CHSH^+ + H + Ar, \quad \Delta H_0^0 = 1.47 \text{ eV}, \tag{4}$$

$$\rightarrow CH_3CH_2^+ + SH + Ar, \quad \Delta H_0^0 = 1.96 \text{ eV}, \tag{5}$$

$$\rightarrow CH_2CH_2^+ + H_2S + Ar, \quad \Delta H_0^0 = 1.97 \text{ eV}, \tag{6a}$$

$$\rightarrow CH_2CH_2^+ + SH + H + Ar, \quad \Delta H_0^0 = 5.87 \text{ eV}, \tag{6b}$$

$$\rightarrow C_2H_3^+ + H_2 + SH + Ar, \quad \Delta H_0^0 = 4.28 \text{ eV}, \tag{7a}$$

$$\rightarrow C_2H_3^+ + H_2S + H + Ar, \quad \Delta H_0^0 = 4.87 \text{ eV}, \tag{7b}$$

$$\rightarrow CH_3^+ + CH_2SH + Ar, \quad \Delta H_0^0 = 4.03 \text{ eV}, \tag{8a}$$

$$\rightarrow CH_3^+ + CH_3S + Ar, \quad \Delta H_0^0 = 5.50 \text{ eV}, \tag{8b}$$

$$\rightarrow CH_3^+ + CH_2 + SH + Ar, \quad \Delta H_0^0 = 7.91 \text{ eV}, \tag{8c}$$

$$\rightarrow CH_2SH^+ + CH_3 + Ar, \quad \Delta H_0^0 = 1.73 \text{ eV}, \tag{9a}$$

$$\rightarrow CH_3S^+ + CH_3 + Ar, \quad \Delta H_0^0 = 3.18 \text{ eV}, \tag{9b}$$

$$\rightarrow CH_2S^+ + CH_4 + Ar, \quad \Delta H_0^0 = 0.92 \text{ eV}, \tag{10a}$$

$$\rightarrow HCSH^+ + CH_4 + Ar, \quad \Delta H_0^0 = 1.10 \text{ eV}, \tag{10b}$$

$$\rightarrow CH_2S^+ + CH_3 + H + Ar, \quad \Delta H_0^0 = 5.40 \text{ eV}, \tag{10c}$$

$$\rightarrow CHS^+ + CH_3 + H_2 + Ar, \quad \Delta H_0^0 = 3.10 \text{ eV}, \tag{11a}$$

$$\rightarrow CHS^+ + CH_3 + 2H + Ar, \quad \Delta H_0^0 = 7.59 \text{ eV}, \tag{11b}$$

$$\rightarrow CHS^+ + CH_4 + H + Ar, \quad \Delta H_0^0 = 4.57 \text{ eV}, \tag{11c}$$

TABLE II. Current recommended experimental $\Delta_f H_0^\circ$ and IE values for CH_3CH_2SH, CH_3CH_2S, CH_2SH, CH_3S, CH_2S, CHS, CH_3, CH_2, CH_3CH_2, CH_2CH_2, C_2H_3, $CH_3CH_2SH^+$, $CH_3CH_2S^+$, CH_3CHSH^+, CH_2SH^+, CH_3S^+, CH_2S^+, $HCSH^+$, CHS^+, CSH^+, and CH_3^+.[a]

Species	$\Delta_f H_0^\circ$ (kcal/mol)	IE (eV)
Neutrals		
gauche-C_2H_5SH	-7.1[b]	9.2927 ± 0.0006[b]
trans-C_2H_5SH	-6.6[b]	...
CH_3CH_2S	31.4 ± 2[c] (27.5)[c,d]	8.97 ± 0.01[c]
CH_2SH	37.7 ± 2.0[e]	7.536 ± 0.003[e]
$CH_3S(^2E_{3/2})$	31.4 ± 0.5[f]	9.2649 ± 0.0010[g]
$CH_3S(^2E_{1/2})$		9.2330 ± 0.0010[g]
CH_2S	28.3 ± 2.0[h]	9.376 ± 0.003[h]
HCS	71.7 ± 2.0[h]	7.412 ± 0.007[h]
CSH	...	...
H_2S	-4.2 ± 0.2	10.4682 ± 0.0002[i]
SH	34.0 ± 0.6[f]	10.4218 ± 0.0004[j]
CH_3CH_2	28	8.13
CH_2CH_2	14.5	10.507 ± 0.004
CH_3	35.6 ± 0.3	9.8380 ± 0.0004[k]
CH_2	93	10.396 ± 0.003
H	51.63	13.598
Cations		
gauche-$C_2H_5SH^+$	207.3[b]	
trans-$C_2H_5SH^+$	207.4[b]	
$CH_3SCH_3^+$	194.1[d]	
$CH_3CHSH_2^+$	220.1[d,e]	
$CH_2CH_2SH_2^+$	220.0[d,e]	
$CH_3CH_2S^+$	236.5[c]	
CH_2SH^+	211.5 ± 2.0[b]	
CH_3S^+	245.0 ± 0.5[f,g]	
CH_2S^+	244.5 ± 2.0[h]	
trans-$HCSH^+$	≈270,[l] 275[d,m]	
cis-$HCSH^+$	≈270,[l] 277[d,m]	
HCS^+	243.2 ± 2.9[h]	
CSH^+	314.6[d,m]	
H_2S^+	237.2 ± 0.2[j,n]	
SH^+	274.3 ± 0.6[f,j]	
$CH_3CH_2^+$	218.5 ± 1	
$CH_2CH_2^+$	256.8	
CH_3^+	262.5 ± 0.3[k,n]	

[a]Unless specified, the values are obtained from Ref. 15.
[b]Reference 10.
[c]Reference 21.
[d]G2 calculation.
[e]Reference 22.
[f]Reference 23.
[g]Reference 11.
[h]Reference 24.
[i]Reference 16.
[j]Reference 17.
[k]Reference 18.
[l]See Refs. 3 and 15.
[m]Reference 25.
[n]Reference 15.

$$\rightarrow H_2S^+ + CH_2CH_2 + Ar,$$
$$\Delta H_0^0 = 1.93 \text{ eV}. \quad (12)$$

By comparison of the observed AE(CID) value for a product ion with the thermochemical thresholds of possible reaction channels, information about the structure of the product ion can be obtained.

The formation of $CH_3CH_2^+ + SH$ is supported by the excellent agreement observed between the AE(CID) value of 1.9 ± 0.2 eV for $CH_3CH_2^+$ and the thermochemical threshold of $\Delta H_0^0 = 1.96$ eV for reaction (5). In the previous CID study of $CH_3SH^+ + Ar$, the formation of $CH_3^+ + SH$, which results from the cleavage of the $CH_3^+ - SH$ bond, has a sharp onset. As shown in Fig. 3(a), the experimental onset for $CH_3CH_2^+$ from the CID reaction of $CH_3CH_2SH^+ + Ar$ is also sharp. These observations are consistent with the interpretation that the formation of CH_3^+ and $CH_3CH_2^+$ from CH_3SH^+ and $CH_3CH_2SH^+$, respectively, involves a direct C–S bond breakage process via a loose transition complex. Since the charge in $CH_3CH_2SH^+$ is mainly located at the S atom, the formation of $CH_3CH_2^+ + SH$ from $CH_3CH_2SH^+$ must involve the charge transfer from the SH^+ moiety to the CH_3CH_2 component during the C–S bond cleavage process. Such a charge transfer process corresponds to a curve crossing between the potential surfaces formed by $CH_3CH_2 + SH^+$ and $CH_3CH_2^+ + SH$. Considering that the IE(SH) $= 10.4219\pm0.0004$ eV (Ref. 17) is significantly higher than the IE(CH_3CH_2) $= 8.13$ eV,[15] the charge transfer from SH^+ to CH_3CH_2 should be an energetically favored process. This may account for the fact that SH^+ is not observed as a CID product.

The AE(CID) value of 2.0 ± 0.2 eV for $C_2H_4^+$ is consistent with the thermochemical threshold $\Delta H_0^0 = 1.97$ eV for reaction 6(a), but significantly lower than that of $\Delta H_0^0 = 5.87$ eV for reaction 6(b). So we may conclude that the formation of $C_2H_4^+$ is accompanied by H_2S at the threshold. At higher $E_{c.m.}$'s, the H-elimination from internally excited $CH_3CH_2^+$ may also contribute to the production of $C_2H_4^+$. Thus, reaction (6b) is a possible source of $C_2H_4^+$ at $E_{c.m.} > 5.9$ eV.

The AE(CID) value determined for the formation of $C_2H_3^+$ is 4.2 ± 0.2 eV and is in accord with the thermochemical threshold of $\Delta H_0^0 = 4.28$ eV for reaction (7a). The thermochemical threshold of $\Delta H_0^0 = 4.87$ eV for the dissociation channel $C_2H_3^+ + H_2S + H$ [reaction (7b)] is slightly higher than the AE(CID) for $C_2H_3^+$. At sufficiently high $E_{c.m.}$'s, excited $C_2H_5^+$ and $C_2H_4^+$ formed in reactions (5) and (6a) might undergo H_2 and H elimination, respectively, to produce $C_2H_3^+$. As shown in Fig. 3(b), the rapid growth of the cross section for $C_2H_3^+$, beginning at $E_{c.m.} \approx 7$ eV, is accompanied by the corresponding drop in the cross section for $C_2H_5^+$ as $E_{c.m.}$ is increased. This observation suggests that the increase in the $C_2H_3^+$ intensity is mostly resulted from the secondary decomposition of excited $C_2H_5^+$ at $E_{c.m.} > 7$ eV.

The AE(CID) value of 1.7 ± 0.2 eV for the mass 47 ion is in excellent agreement with the thermochemical threshold of $\Delta H_0^0 = 1.73$ eV for reaction (9a), indicating that CH_2SH^+ is formed near the CID onset for the mass 47 ion. To confirm this structure for the mass 47 ion, we have performed the charge transfer probing experiment using the double RFOIGGC scheme described in the Experiment. On the basis of the energetics for reactions (1) and (2), we expect to observe $C_6H_6^+$ if the mass 47 ion has the CH_3S^+ structure, whereas no $C_6H_6^+$ ions should be produced if the mass 47 ion possesses the CH_2SH^+ structure. Since no charge transfer product $C_6H_6^+$ ions were observed, we conclude that the mass 47 ions formed in the CID reaction of $CH_3CH_2SH^+ + Ar$ at $E_{c.m.} = 1.7$–5.0 eV have indeed predominantly the CH_2SH^+ structure. The thermochemical threshold of 3.18 eV for the

formation of $CH_3S^+ + CH_3$ [reaction (9b)] is considerably higher than that of reaction (9a).

A very weak onset is observed at AE(CID) $= 1.5 \pm 0.4$ eV for the CH_2S^+ ion. Although this value is higher than the thermochemical threshold of $\Delta H_0^0 = 0.92$ eV for reaction (10a), we conclude that $CH_2S^+ + CH_4$ is formed at the AE-(CID) for CH_2S^+. The thermochemical threshold for the formation of $CH_2S^+ + CH_3 + H$ [reaction (10c)] is $\Delta H_0^0 = 5.40$ eV, suggesting that excited CH_2SH^+ may be the precursor of CH_2S^+ at $E_{c.m.} > 5.4$ eV. The formation of *cis*-$HCSH^+$ (and/or *trans*-$HCSH^+$) (Ref. 22) together with CH_4 [reaction (10b)], which has a thermochemical threshold of ≈ 1.1 eV, is also a viable process.

The onset for HCS^+ is very gradual, indicating that this ion may be produced by a stepwise dissociation mechanism or via a tight transition complex. The upper limit of the AE-(CID) for HCS^+ is estimated to be 7.2 ± 0.5 eV, which is significantly higher than the ΔH_0^0 values of 3.1 and 4.57 eV for reactions (11a) and (11c), respectively. The formation of HCS^+ may involve the further dissociation of excited CH_2SH^+ and/or CH_2S^+. We note that the $\Delta_f H_0^0$ for CSH^+ is 3.1 eV higher than that for HCS^+ (see Table II). The formation of CSH^+ at higher $E_{c.m.}$'s cannot be excluded.

The cross section for CH_3^+ is on average the lowest in the $E_{c.m.}$ range of interest here. The cross section curve for CH_3^+ has a weak onset at 3.8 ± 0.3 eV and exhibits a plateau in the $E_{c.m.}$ range of 4–8 eV. At $E_{c.m.} \approx 8$ eV, the cross section for CH_3^+ begins to rise gradually as $E_{c.m.}$ is increased. Since the AE(CID) for CH_3^+ is in good agreement with the thermochemical threshold of $\Delta H_0^0 = 4.03$ eV for reaction (8a), we conclude that the breakage of the $CH_3^+ - CH_2SH$ bond to form CH_3^+ and CH_2SH does not have a potential barrier. Although the charge of $CH_3CH_2SH^+$ is originally located at the S atom, the charge may hop from CH_2SH^+ to CH_3 during the cleavage of the C–C bond in $CH_3CH_2SH^+$. Since the IE of CH_2SH (7.536 ± 0.003 eV) (Ref. 22) is substantially lower than the IE of CH_3 (9.8380 ± 0.0004 eV),[18] we expect that the formation of $CH_3^+ + CH_2SH$ is not favorable. We note that the thermochemical threshold for the formation of $CH_3^+ + CH_2 + SH$ [reaction (8c)] is $\Delta H_0^0 = 7.91$ eV, which appears to coincide with the further increase in cross section for CH_3^+ at $E_{c.m.} \approx 8$ eV. A finite contribution to the formation of CH_3^+ at $E_{c.m.} > 8$ eV may arise from the further dissociation of $CH_3CH_2^+$.

The AE(CID) for H_2S^+ is determined to be 2.0 ± 0.3 eV, indicating that reaction (12) is responsible for the formation of H_2S^+ at the onset. The *ab initio* calculations suggest that $C_2H_4^+$ and H_2S^+ are formed via a $CH_2CH_2SH_2^+$ intermediate (see Sec. III C below). Due to the similar IE for H_2S (10.4682 ± 0.0002 eV) (Ref. 16) and CH_2CH_2 (10.507 ± 0.004 eV),[15] the intensities for product H_2S^+ and $CH_2CH_2^+$ are expected to be similar. This expectation is consistent with the similar cross sections observed for H_2S^+ and $C_2H_4^+$.

Figure 4(a) shows the relative abundances in percentage for the observed CID product ions $C_2H_5^+$, $C_2H_4^+$, $C_2H_3^+$, CH_3^+, CH_2SH^+, CH_2S^+, CHS^+, and H_2S^+ in the $E_{c.m.}$ range of 2–42 eV. Here, the sum of the abundances for all product ions at a specific $E_{c.m.}$ is normalized to 100%. Due to the poor signal to noise ratios for the cross section data at $E_{c.m.} < 2$ eV, the relative abundance data at this $E_{c.m.}$ range are not included in Fig. 4(a). The relatively abundance of $C_2H_5^+$ reaches a plateau at 3–6 eV and decreases monotonically from 63% to 20% as $E_{c.m.}$ is increased from 6 eV to 42 eV. The decrease of the relative abundance for $C_2H_5^+$ appears to coincide with the increase in the relative abundance for $C_2H_3^+$, suggesting that a finite fraction of excited $C_2H_5^+$ ions initially formed at $E_{c.m.} > 7$ eV further decomposes by H_2-elimination to produce $C_2H_3^+$. Over the $E_{c.m.}$ range of 2–42 eV, the relative abundance of CH_2SH^+ remains constant at $\approx 25\%$. The relative abundances for $C_2H_5^+$, CH_2SH^+, and $C_2H_3^+$ become nearly the same at $E_{c.m.} = 25$–42 eV. The relative abundance for CH_2S^+ decreases from 15% to 5% as $E_{c.m.}$ is increased from 2 eV to 14 eV, and gradually increases again from 5% to 10% as $E_{c.m.}$ is further increased to 42 eV. The relative abundences for other minor product ions are found to be $< 10\%$ over the entire $E_{c.m.}$ range. We expect that the relative abundances for all product ions become similar at high $E_{c.m.}$'s (> 30 eV) that

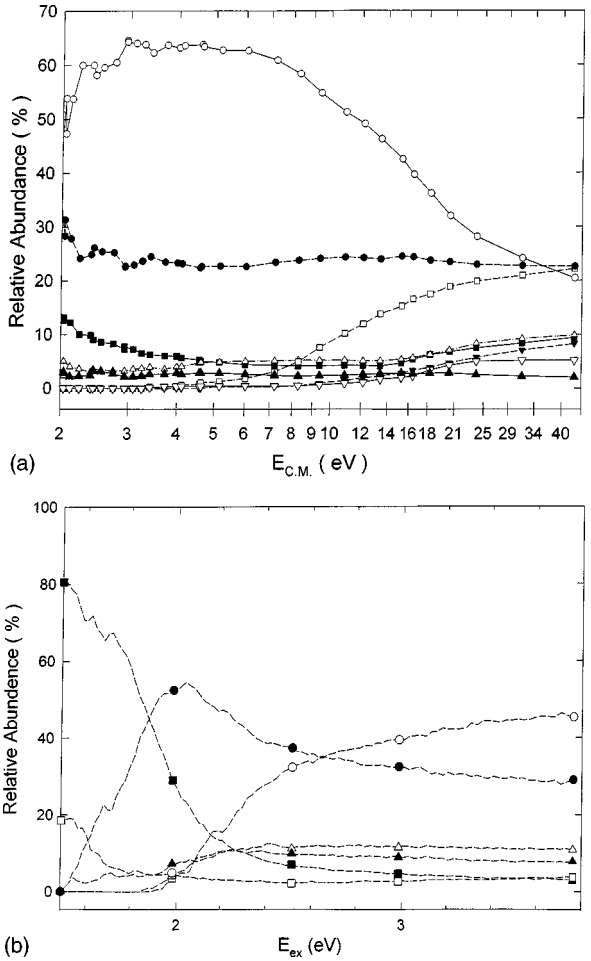

FIG. 4. (a) Relative abundances in percentage for $CH_3CH_2^+$ (○), $C_2H_4^+$ (△), $C_2H_3^+$ (□), CH_2SH^+ (CH_3S^+) (●), CH_2S^+ (■), HCS^+ (▼), CH_3^+ (▽), and H_2S^+ (▲) formed in the CID reaction of $CH_3CH_2SH^+ + Ar$ at $E_{c.m.} = 2$–42 eV. (b) Relative abundances in percentage for CH_3CHSH^+ (□), $CH_3CH_2^+$ (○), $C_2H_4^+$ (△), CH_2SH^+ (CH_3S^+) (●), CH_2S^+ (■), and H_2S^+ (▲) formed in the PI of CH_3CH_2SH. The sum of all the product ions is arbitrarily set to 100%.

are significantly higher than the endothermicities of the dissociation reactions (3)–(12).

B. Photoionization efficiency spectra for fragment ions from CH_3CH_2SH

We have measured the PIE spectra (not shown here) for ions from CH_3CH_2SH in the wavelength range of 1350–950 Å using a wavelength resolution of 5 Å (FWHM). The photoions observed are $CH_3CH_2SH^+$, $C_2H_5S^+$, $C_2H_5^+$, $C_2H_4^+$, $CH_2SH^+(CH_3S^+)$, CH_2S^+, and H_2S^+.

In the PI experiment, fragment ions can be considered as produced by the unimolecular dissociation of excited $CH_3CH_2SH^+$ ions initially formed by the PI of CH_3CH_2SH. The maximum excitation energy (E_{ex}) acquired by $CH_3CH_2SH^+$ thus formed can be calculated as $E_{ex}=h\nu-\mathrm{IE}(CH_3CH_2SH)$. The AE(CID) value can be compared directly to $\Delta(\mathrm{PI})=\mathrm{AE(PI)}-\mathrm{IE}(CH_3CH_2SH)$, where AE(PI) is the AE for a fragment ion observed in PI. The Δ(PI) values for the photoions $C_2H_5S^+$, $C_2H_5^+$, $C_2H_4^+$, $CH_2SH^+(CH_3S^+)$, CH_2S^+, and H_2S^+ are in good agreement with the corresponding AE(CID) values (see Table I). It is known that $C_2H_5S^+$ can exist in several isomeric structures.[19] On the basis of the Δ(PI) value of 1.47 ± 0.06 eV for $C_2H_5S^+$, we conclude that CH_3CHSH^+ is formed at the PI threshold for $C_2H_5S^+$. We have also probed the structure for the mass 47 ion formed in the PI of CH_3CH_2SH by examining its charge transfer reaction with benzene. The fact that no charge transfer product $C_6H_6^+$ ions were observed indicates that the mass 47 ions formed in the PI of CH_3CH_2SH have predominantly the CH_2SH^+ structure.

Figure 4(b) shows the relative abundances of the fragment ions CH_3CHSH^+, $C_2H_5^+$, $C_2H_4^+$, CH_2SH^+, CH_2S^+, and H_2S^+ observed in the PI of CH_3CH_2SH in the E_{ex} range of 1.5–3.8 eV. Here, the sum of the abundances for all photoions except for that for $CH_3CH_2SH^+$ is normalized to 100%. The high abundances for CH_2S^+ and CH_3CHSH^+ at $E_{ex}<1.7$ eV are consistent with the fact that $CH_2S^++CH_4$ and CH_3CHSH^++H are the only two energetically allowed dissociation channels in this $E_{c.m.}$ range. The formation of $CH_2S^++CH_4$ necessarily involves a tight transition complex. Thus, we expect that the intensities for $C_2H_5^+$ and CH_2SH^+, which are formed by a simple bond cleavage process, overtake that for CH_2S^+ at higher $E_{c.m.}$'s. This expectation is confirmed by the relative abundance data of Fig. 4(b), showing that CH_2SH^+ is the dominant product ion at $E_{ex}\approx1.8$–2.8 eV, while $C_2H_5^+$ becomes the major product ion at $E_{ex}>2.8$ eV. Although the relative abundance curves obtained by the PI of CH_3CH_2SH are not energy-selected data, it is interesting to note that the E_{ex} dependencies of these relative abundance curves are in qualitative accord with the statistical QET predictions.

Comparing the relative abundance data plotted in Figs. 4(a) and 4(b), we note two major differences. First, the CH_3CHSH^+ ion observed in the PI of CH_3CH_2SH is not found in the CID study. The other difference is that the relative abundance curves for $C_2H_5^+$, CH_2SH^+, and CH_2S^+ observed in PI exhibit a stronger E_{ex} dependence than that measured in the CID of $CH_3CH_2SH^+$. At $E_{ex}\approx2$–2.8 eV, $C_2H_5^+$ formed in the PI of CH_3CH_2SH is not the dominant ion, contrary to the CID results.

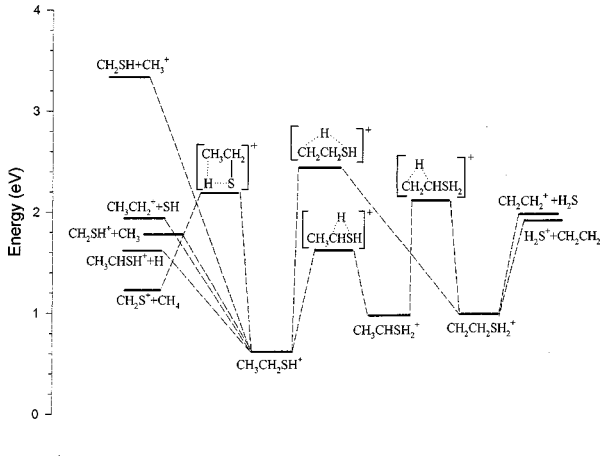

FIG. 5. Schematic of the potential-energy profile for rearrangement and dissociation reactions for $CH_3CH_2SH^+$. The energies for the transition structures and product channels are based on G2 calculations and experimental $\Delta_f H_0^0$ values listed in Table I. See the text. The transition structures are predicted to exist and are shown in square brackets. However, the detailed structures for the transition structures are not given here.

C. Theoretical potential-energy profile for the unimolecular reactions of $CH_3CH_2SH^+$

In order to rationalize the dissociation pathways observed in this study, we have also investigated the transition structures and their energetics involved in the unimolecular reactions of $CH_3CH_2SH^+$ using the *ab initio* GAUSSIAN-2 (G2) theoretical procedures.[1,25] The calculated potential-energy profiles for possible rearrangement and dissociation pathways leading to the formation of CH_3CHSH^+, $CH_3CH_2^+$, $C_2H_4^+$, CH_2SH^+, CH_2S^+, H_2S^+, and CH_3^+ are depicted in Fig. 5.

The dissociation reactions of $CH_3CH_2SH^+$ to form CH_3CHSH^++H, $CH_3CH_2^++SH$, $CH_2SH^++CH_3$, and $CH_3^++CH_2SH$, which involve the respective cleavage of a single C–H, C–S, and C–C bond, are predicted to have no potential barriers. These theoretical predictions are consistent with the experimental observation that the AE(CID) and Δ(PI) for these product channels agree with their corresponding thermochemical thresholds. If the elimination of CH_4 from $CH_3CH_2SH^+$ proceeds via a one-step process, it is predicted to involve a four-center cyclic transition structure lying 2.31 eV above the energy for $CH_3CH_2SH^+$ as shown in Fig. 5. We note that the AE(CID) value of 1.5 ± 0.4 eV for CH_2S^+ is higher than the thermochemical threshold of $\Delta H_0^0=0.92$ eV for the formation of $CH_2S^++CH_4$ from reaction (10a). The Δ(PI) value 1.42 ± 0.06 eV for CH_2S^+ observed in the PI experiment is close to the AE(CID) value. These observations suggest a potential energy barrier of ≈0.6 eV above the energy of the $CH_2S^++CH_4$ channel. However, the theoretical barrier is ≈0.8 eV higher than the experimental barrier.

By a 1,2-H (1,3-H) shift, the $CH_3CH_2SH^+$ ion may rearrange to form the $CH_3CHSH_2^+$ ($CH_2CH_2SH_2^+$) isomeric structure. The $CH_3CHSH_2^+$ and $CH_2CH_2SH_2^+$ isomers are predicted to be stable with energies lying 0.55 and 0.54 eV,

respectively, above the parent $CH_3CH_2SH^+$. The transition structure that interconverts $CH_3CH_2SH^+$ and $CH_3CHSH_2^+$ by the 1,2-H shift is located to be 1.5 eV higher in energy with respect to that for $CH_3CH_2SH^+$, whereas the transition structure that allows the interconversion of $CH_3CH_2SH^+$ and $CH_2CH_2SH_2^+$ by a 1,3-H shift lies 2.71 eV above the parent $CH_3CH_2SH^+$. The dissociation of $CH_2CH_2SH_2^+$ to yield $CH_2CH_2^+ + H_2S$ and $H_2S^+ + CH_2CH_2$ is predicted to have no reaction barriers. Thus, the overall potential barrier for the dissociation from $CH_3CH_2SH^+$ to form $CH_2CH_2^+ + H_2S$ and $H_2S^+ + CH_2CH_2$ is governed by the barrier for the conversion between $CH_3CH_2SH^+$ and $CH_2CH_2SH_2^+$. The fact that the AE(CID) and Δ(PI) values for $C_2H_4^+$ and H_2S^+ agree with the thermochemical thresholds for the formation of $CH_2CH_2^+ + H_2S$ and $H_2S^+ + CH_2CH_2$ indicates that the potential barrier for the arrangement of $CH_3CH_2SH^+$ to $CH_2CH_2SH_2^+$ is ≈ 2.0 eV. The latter value is lower than the theoretical barrier by ≈ 0.7 eV.

The formation of $CH_2CH_2SH^+$ from $CH_3CH_2SH^+$ can be achieved by two 1,2-H shifts, i.e., $CH_3CH_2SH^+ \rightarrow CH_3CHSH_2^+ \rightarrow CH_2CH_2SH_2^+$. If the second 1,2-H shift, which converts $CH_3CHSH_2^+$ into $CH_2CH_2SH_2^+$, has a similar potential barrier as that (1.5 eV) for the arrangement from $CH_3CH_2SH^+$ to $CH_3CHSH_2^+$, we expect an overall potential barrier of ≈ 2.05 eV with respect to the energy of $CH_3CH_2SH^+$. Such a value would be closer to the experimental barrier. With this expectation in mind, we have located the transition structure for the second 1,2-H shift between the terminal and middle C atoms. The G2 energy for this transition structure yields an effective barrier of 2.26 eV above the energy of $CH_3CH_2SH^+$. This calculated barrier is still slightly higher than the experimental value of 2.0 ± 0.2 eV. Taking into account the experimental uncertainties, we consider the theoretical barrier of 2.26 eV associated with the stepwise 1,2-H shift mechanism to be in reasonable accord with the experimental results.

The formation of CHS^+ can be accomplished by the further elimination of H_2 and H from product CH_2SH^+ and CH_2S^+, respectively. These stepwise pathways (not shown in Fig. 5), which result in the formation of $CHS^+ + H_2 + CH_3$ and $CHS^+ + H + CH_4$, are predicted to proceed without a potential barrier.

D. Dissociation mechanisms for collision-activated $CH_3CH_2SH^+$

The two basic assumptions of the statistical QET are that a critical configuration or transition state controls the reaction rate, and that the internal energy is randomly distributed in the molecule's active degrees of freedom. These assumptions lead to the conclusion that the most favorable product corresponds to the most stable product channel provided that a tight transition structure is not involved. As pointed out above, the formation of $CH_2S^+ + CH_4$ [reaction (10a), $\Delta H_0^0 = 0.92$ eV] from $CH_3CH_2SH^+$ involves a tight transition complex. The formation of the other major product channels $CH_3CHSH^+ + H$ [reaction (4), $\Delta H_0^0 = 1.47$ eV], $CH_3CH_2^+ + SH$ [reaction (5), $\Delta H_0^0 = 1.96$ eV], and $CH_2SH^+ + CH_3$ [reaction (9a), $\Delta H_0^0 = 1.73$ eV], which involve the breakage of the C–H, C–S, and C–C bonds, respectively, in $CH_3CH_2SH^+$, is expected to proceed via a loose transition structure and to have no potential energy barriers. Since the endothermicities for reactions (4) and (9a) are lower than reaction (5), we expect that CH_2SH^+ and CH_3CHSH^+ are among the major product ions. The observation that $CH_3CH_2^+$ [reaction (5)] is the dominant product channel for the CID reaction of $CH_3CH_2SH^+ + Ar$ over the $E_{c.m.}$ range of 2–30 eV is most interesting. This, together with the fact that CH_3CHSH^+ is not observed as a CID product ion, suggests that the CID reaction of $CH_3CH_2SH^+ + Ar$ is not compatible with the statistical QET predictions.

In the $E_{c.m.}$ range of this CID experiment, the collisions are most efficient for the promotion of translation-vibration and translation-rotation energy exchanges. However, electronic excitation by low energy collisions is highly inefficient. In the previous CID study of the $CH_3SH^+ + Ar$ system, the observation that the formation of $CH_3^+ + SH$ dominates the more stable product channel $CH_2SH^+ + H$ is contrary to the QET prediction. The highest vibrational frequencies of CH_3SH^+ correspond to the C–H and SH stretching vibrational modes with harmonic frequencies of $\approx 3000\ cm^{-1}$, while the C–S stretching frequency of $687\ cm^{-1}$ is the second lowest.[1,2,26] Fenn *et al.* argue that the internal vibrational excitation of $CH_3CH_2SH^+$ resulting from the low energy collision with Ar is predominantly deposited in the C–S stretching mode instead of the C–H or S–H stretching modes of CH_3SH^+.[2] Owing to the large difference in vibrational frequencies between the C–S and C–H (S–H) stretching modes of CH_3SH^+, the C–S and C–H (or S–H) stretching modes are only weakly coupled, i.e., the energy flow between the C–S and C–H (or S–H) vibrational modes of CH_3SH^+ is inefficient. As a consequence, the product CH_3^+ ion, which results from the C–S bond cleavage, is favored over the product CH_2SH^+ ion associated with the cleavage of the $H–CH_2SH^+$ bond.

This CID study of $CH_3CH_2SH^+ + Ar$ can be considered a test for the physical picture gained in the CID experiment $CH_3SH^+ + Ar$. Based on the recent experimental and *ab initio* calculations,[10] the stretching frequencies associated with the C–H, S–H, and C–S bonds of $CH_3CH_2SH^+$ are similar to those of CH_3SH^+.[26] The C–C stretching mode of $CH_3CH_2SH^+$ has a frequency of $\approx 1000\ cm^{-1}$,[2,10] although higher than the C–S stretching frequency of $617\ cm^{-1}$, but significantly lower than the C–H (S–H) stretching frequencies. In addition to the more efficient collision excitations of the C–S and C–C stretching modes, the coupling between the C–S and C–C vibrational modes of $CH_3CH_2SH^+$ should also be more efficient. Owing to the large frequency difference between the C–S(C–C) and C–H(S–H) stretching modes, the coupling or energy flow between the C–S (C–C) and C–H (S–H) stretching modes is also expected to be small within the time scale of the dissociation. As a consequence, product channels arising from the cleavage of the C–S and C–C bonds may dominate in the collisional-activated dissociation of $CH_3CH_2SH^+$. This expectation is confirmed by the dominant abundances of the $CH_3CH_2^+$ and CH_2SH^+ ions observed in the present CID experiment. The failure to observe the formation of CH_3CHSH^+, which cor-

responds to a more stable product channel, can be attributed to the inefficient energy flow between the C–H and C–S(C–C) stretching modes. These results suggest that the CID reaction of $CH_3CH_2SH^+ + Ar$ is not consistent with the QET predictions.

A strong bond is usually associated with a high stretching vibrational frequency. Although the C–H stretching frequencies for CH_3SH^+ and $CH_3CH_2SH^+$ are typical of a C–H bond, the D_0 values for the $H–CH_2SH^+$ and $H–CH(CH_3)SH^+$ bonds are significantly lower than that of a normal C–H bond. This is due to the energy gained in the formation of the $CH_3CH{=}SH^+$ double bond as the H-atom is departing from the middle C atom of $CH_3CH_2SH^+$. As pointed out previously by Chen *et al.*,[1] the high frequency and weak bond dissociation energy scenario is a key feature for the observed bond selective collisional-activated dissociation of CH_3SH^+ and $CH_3CH_2SH^+$.

The nature of fragment ions and their relative abundances observed in previous PI (Ref. 3) and charge exchange[4] studies of CH_3SH are in qualitative agreement with predictions of the statistical QET. Similar to this observation, we also find that the nature of fragment ions and their relative abundances measured in the PI of CH_3CH_2SH are in qualitative accord with the QET predictions, indicating that the energy randomization assumption is mostly valid when the internal energy of $CH_3CH_2SH^+$ is deposited by electronic excitation. As argued in the previous CID study of CH_3SH^+,[2] due to the delocalizated nature of electronic wave functions, an ionization process is capable of inducing finite excitation of the vibrational modes involving the C–S (C–C) as well as the C–H (S–H) bond, and thus will promote better couplings or energy flow between all the vibrational modes. As a result, the dissociation of CH_3SH^+ and $CH_3CH_2SH^+$ behaves statistically.

IV. CONCLUSION

We have examined the relative abundances for $CH_3CH_2^+$, $C_2H_4^+$, $C_2H_3^+$, CH_3^+, CH_2SH^+, CH_2S^+, CHS^+, and H_2S^+ formed in the CID reaction of $CH_3CH_2SH^+ + Ar$ in the $E_{c.m.}$ range of 1–42 eV. The $CH_3CH_2^+ + SH$ channel is found to dominate over this entire $E_{c.m.}$ range. Furthermore, CH_3CHSH^+ was not observed as a CID product ion. Stemming from the fact that the D_0 value for the $CH_3CH_2^+–SH$ bond is greater than that of the $H–CH(CH_3)SH^+$ bond, this observation suggests nonstatistical behavior in the CID of $CH_3CH_2SH^+ + Ar$. In effect, this system, together with the CID reaction of $CH_3SH^+ + Ar$, is an example of bond selective dissociation via collisional activation. Similar to the observation of previous PI studies of CH_3SH, the results of this dissociative PI study of $CH_3CH_2SH^+$ also agree qualitatively with the statistical QET predictions.

The present CID results support the physical picture gained in the previous study of $CH_3SH^+ + Ar$. The dominant production of $CH_3CH_2^+ + HS$ and $CH_3 + CH_2SH^+$ is attributed to the more efficient excitation of the C–S and C–C stretching modes compared to the C–H and S–H stretching modes in the collisional activation of $CH_3CH_2SH^+$. The failure to observe product ions resulting from C–H bond cleavage is rationalized by the inefficient intramolecular energy flow due to weak couplings between the C–S (C–C) and CH_3 (SH) stretching modes of $CH_3CH_2SH^+$.

ACKNOWLEDGMENTS

W.K.L. acknowledges the support of a Research Grants Council (Hong Kong) Earmarked Grant for Research (Account No. 22160080) and a direct grant (Account No. 220600880) from the Chinese University of Hong Kong. Y.J.C. acknowledges the 1997 research Award of Iowa State University. S.S. was the recipient of the GAANN Fellowship for 1994–1995 and 1996–1997. Ames Laboratory is operated for the U.S. Department of Energy by Iowa State University under Contract No. W-7405-Eng-82. This article was supported by the Division of Chemical Sciences, Office of Basic Energy Sciences.

[1] Y.-J. Chen, P. T. Fenn, S. Stimson, and C. Y. Ng, J. Chem. Phys. **106**, 8274 (1997).
[2] P. T. Fenn, Y.-J. Chen, S. Stimson, and C. Y. Ng, J. Phys. Chem. **101**, 6513 (1997).
[3] R. E. Kutina, A. K. Edwards, and J. Berkowitz, J. Chem. Phys. **77**, 5508 (1974).
[4] B.-Ö. Jonsson and J. Lind, J. Chem. Soc., Faraday Trans. 2 **70**, 1399 (1974).
[5] *Handbook of Helium I Photoelectron Spectra of Fundamental Organic Molecules*, edited by K. Kimura, S. Katsumata, Y. Achiba, T. Yamazaki, and S. Iwata (Halsted, New York, 1981).
[6] J.-D. Shao and C. Y. Ng, J. Chem. Phys. **84**, 4317 (1986); J.-D. Shao, Y.-G. Li, G. D. Flesch, and C. Y. Ng, *ibid.* **86**, 170 (1987); G. D. Flesch and C. Y. Ng, *ibid.* **94**, 2372 (1991); G. D. Flesch, S. Nourbakhsh, and C. Y. Ng, *ibid.* **92**, 3490 (1990); G. D. Flesch and C. Y. Ng, *ibid.* **92**, 3235 (1990).
[7] C. Y. Ng, in *State-Selected and State-to-State Ion–Molecule Reaction Dynamics: I. Experiment*, edited by C. Y. Ng and M. Baer (Wiley, New York, 1992); Adv. Chem. Phys. **82**, 401 (1992).
[8] X. Li, Y.-L. Huang, G. D. Flesch, and C. Y. Ng, Rev. Sci. Instrum. **65**, 3724 (1994); **66**, 2871 (1995).
[9] H. M. Gibbs and E. D. Cummins, Rev. Sci. Instrum. **37**, 1385 (1966).
[10] Y.-S. Cheung, C.-W. Hsu, C. Y. Ng, J.-C. Huang, W.-K. Li, and S.-W. Chiu, Int. J. Mass Spectrom. Ion Processes **159**, 13 (1996).
[11] C.-W. Hsu and C. Y. Ng, J. Chem. Phys. **101**, 5596 (1994).
[12] B. Ruscic and J. Berkowitz, J. Chem. Phys. **97**, 1818 (1992).
[13] R. G. Neuhauser, K. Siglow, and H. J. Neusser, J. Chem. Phys. **106**, 896 (1997).
[14] X. Li, Ph.D. thesis, Iowa State University, 1996.
[15] S. G. Lias, J. E. Bartmess, J. L. Holmes, R. D. Levin, and W. G. Mallard, J. Phys. Chem. Ref. Data **17**, Suppl. 2 (1988).
[16] I. Fisher, A. Lochschmidt, A. Strobel, G. Niedner-Schatteburg, K. Müller-Dethlefs, and V. E. Bondybey, J. Chem. Phys. **98**, 3592 (1993).
[17] C.-W. Hsu, D. P. Baldwin, C.-L. Liao, and C. Y. Ng, J. Chem. Phys. **100**, 8047 (1994).
[18] J. A. Bush, P. Chen, R. T. Weimann, and M. G. White, J. Chem. Phys. **98**, 3557 (1993).
[19] C. Y. Ng, in *The Structure, Energetics, and Dynamics of Organic Ions*, Wiley Series in Ion Chemistry and Physics, edited by T. Baer, C. Y. Ng, and I. Powis (Wiley, Chichester, 1996), p. 35.
[20] C. Y. Ng, Adv. Photochem. **22**, 1 (1997).
[21] Z.-X. Ma, C.-L. Liao, H.-M. Yin, C. Y. Ng, S.-W. Chiu, N. L. Ma, and W.-K. Li, Chem. Phys. Lett. **213**, 250 (1993).
[22] B. Ruscic and J. Berkowitz, J. Chem. Phys. **97**, 1818 (1992).
[23] J. M. Nicovich, K. D. Kreutter, C. A. van Dijk, and P. H. Wine, J. Phys. Chem. **96**, 2516 (1992).
[24] B. Ruscic and J. Berkowitz, J. Chem. Phys. **98**, 2568 (1993).
[25] L. A. Curtiss, K. Rahavachari, G. W. Trucks, and J. A. Pople, J. Chem. Phys. **94**, 7221 (1991).
[26] S.-W. Chiu, W.-K. Li, W.-B. Tzeng, and C. Y. Ng, J. Chem. Phys. **97**, 6557 (1992).